

Polyoxometalates

Deutsche Ausgabe: DOI: 10.1002/ange.201510954
Internationale Ausgabe: DOI: 10.1002/anie.201510954Grafting of Secondary Diolamides onto $[P_2W_{15}V_3O_{62}]^{9-}$ Generates Hybrid Heteropoly Acids

David Lachkar, Debora Vilona, Elise Dumont,* Moreno Lelli,* and Emmanuel Lacôte*

Abstract: The Dawson tungstovanadate $[P_2W_{15}V_3O_{62}]^{9-}$ can be grafted to secondary diolamides. The electron-withdrawing character of the polyanion increases the acidity of the amide proton, leading to an organo-polyoxometalate, which can be used as a Brønsted organocatalyst. High-field NMR and DFT modeling indicate that the amide proton stays on the nitrogen and that the exalted acidity derives from the interaction between the organic and inorganic parts of the organo-polyoxometalate. The amide-inserted vanadotungstates thus form a new family of (hybrid) heteropolyacids, offering new perspectives for the application of POM-based catalysis in organic synthesis.

Polyoxometalates (POMs) are nanometric polyanionic clusters, where highly oxidized early transition metals—typically W^{VI} , V^V , or Mo^{VI} —are bound by oxido bridges. The stability of these polyanions makes their protonated forms—called heteropoly acids—highly acidic. Heteropoly acids are widely used catalysts. They can be employed in heterogeneous catalysis, in industrial processes, and scores of other applications.^[1] However, their structural diversity and tunability is relatively narrow and they also have a limited solubility in organic solvents. Thus, their use with sensitive organic substrates remains limited.^[2] New families of heteropoly acids and new strategies to generate them would thus be welcome.

In that context, POM organo-hybrids are especially attractive. They combine the properties of the POMs and the great structural space of organic structures, which can be used to install new properties on POMs, or to tune existing

ones.^[3] One approach focused on the generation of mixed salts from the fully inorganic heteropoly acids and more or less complex amines.^[4] This had led to very efficient systems. However, the POM itself plays no significant role in what essentially are organocatalytic reactions with complex counterions.

To create truly hybrid heteropoly acids in which activity derives from the orbital interplay between the inorganic and organic parts, we considered the potential of Dawson tungstovanadate $[P_2W_{15}V_3O_{62}]^{9-}$. This polyanion can be derivatized by diolamides to generate conjugated organo-POMs.^[5] POM/organic electronic communication is enabled by the insertion of the carbonyl into the polyoxometallic structure. We surmised that since POMs are good electron reservoirs, they might stabilize the anions derived from deprotonation of the amide on the hybrid structures by accepting the extra negative charge of the conjugated amide. This delocalization of the conjugated charge over the whole POM would thus increase the acidity of the amide (Figure 1). With the help of high-field NMR and computational modeling we show here that this is the case.

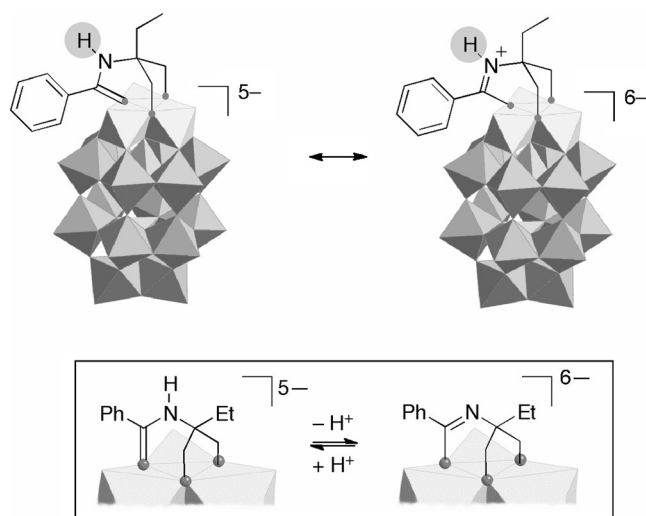


Figure 1. Deprotonation of the POM-diols.

The phenyl (**1a**), *p*-nitro (**1b**) and *p*-methoxy (**1c**) derivatives have been previously prepared in our group (Figure 2).^[5a] We added electron-poor *p*-trifluoromethyl **1d** to the array of POMs. Together, these four representative POMs (with the general formula $TBA_3[P_2W_{15}O_{59}\{(OCH_2)_2C(Et)NHC(=O@POM)R\}]$) cover the whole range of electronic effects on the conjugated aromatic ring, which might

[*] D. Lachkar, Dr. E. Lacôte

ICSN CNRS

1 avenue de la Terrasse, 91198 Gif-sur-Yvette Cedex (France)

D. Vilona, Dr. E. Lacôte

Univ Lyon, CPE Lyon, Université Claude Bernard Lyon1, CNRS,

Institut de chimie de Lyon, C2P2 UMR 5265

69616 Villeurbanne (France)

E-mail: emmanuel.lacote@univ-lyon1.fr

D. Vilona, Dr. M. Lelli

Univ Lyon, Université Claude Bernard Lyon1, ENS Lyon, CNRS,

Institut de chimie de Lyon, ISA-CRMN UMR 5280

69100 Villeurbanne (France)

E-mail: moreno.elli@ens-lyon.fr

D. Vilona, Dr. E. Dumont

Univ Lyon, ENS de Lyon, CNRS, Université Lyon 1, Laboratoire de

chimie, UMR 5182

69342 Lyon (France)

E-mail: elise.dumont@ens-lyon.fr

Supporting information for this article can be found under:
<http://dx.doi.org/10.1002/ange.201510954>.

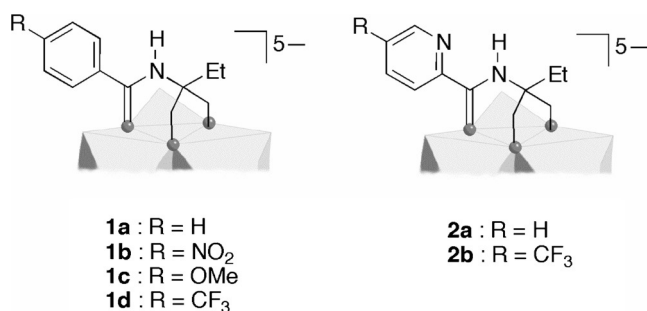


Figure 2. TBA₅[P₂V₃W₁₅O₅₉]{(OCH₂)₂C(Et)NHC(=O@POM)R} organo-POMs considered in this work.

influence the acidity. POM **1d** was prepared in 99% yield using our established method. We also prepared pyridine derivatives **2a,b**,^[5c] which have an internal basic site.

The most noticeable feature of POMs **1a–d** is the chemical shift of the proton of the grafted amide in CD₃CN. It ranges from 9.15 ppm for **1c** to 9.86 ppm for **1b**, with POM **1a** at 9.32 ppm and **1d** at 9.68 ppm. The chemical shift for **2a** and **2b** is 10.40 ppm. This suggests that the iminium resonance form of the amide might be stabilized by the POM structure. However, it might also be possible that the amide would be deprotonated, and the proton released would remain on the POM as a counterion. To discriminate between these two options, we decided to monitor the amide resonance with 2D ¹H-¹⁵N HSQC experiments at natural nitrogen isotopic abundance (see Supporting Information for details) on POMs **1a, 2a,b**.

Figure 3 shows the overlap of the HSQC spectra acquired on the POMs. Strong cross-peaks were observed for the amide with a ¹⁵N chemical shift of about 160 ppm and ¹H chemical shifts ranging from 9.4 for **1a** to 10.4 ppm for **2a** and **2b**. In the same spectrum, we also observed weak cross-peaks at around 120 ppm for nitrogen and 6.9 ppm for **1a**, 8.6–8.7 ppm

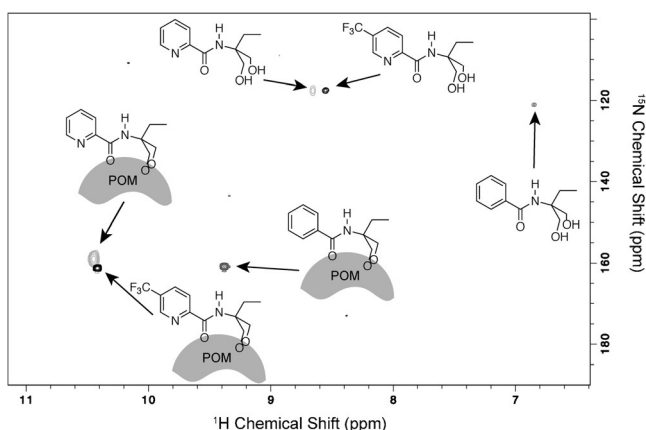


Figure 3. Superposition of the ¹H-¹⁵N HSQC spectra of the hybrid-POM solution in CD₃CN (**1a**: 5 mM, **2a**: 2.3 mM, **2b**: 7.5 mM; T = 298 K). The spectra were acquired at 14.1 T (600 and 60.8 MHz for ¹H and ¹⁵N respectively) using 512 × 128 complex points with 64 scans, 4.0 s of recycle delay, and FID acquisition times of 17.5 ms and 53.2 ms in the indirect and direct dimension, respectively. The 2D FID was processed with a 1024 × 512 complex matrix points with square-cosine windows functions for both the direct and indirect dimensions.

for **2a,b**. Comparison with authentic samples showed that the latter corresponded to remaining traces of the free diolamide ligands of **1a, 2a,b** that did not get anchored to the POM scaffold. In both the free diolamides and the organo-POMs, the proton resonances of the amide in the pyridine derivatives are from 1 to 1.5 ppm downfield compared to their analogous benzamide derivative. In the ¹H-¹⁵N HSQC experiments one can only observe the ¹⁵N resonance of atoms that are directly bound to a proton. Thus there is no cross peak corresponding to the pyridine nitrogen of **2a** and **2b**. The ¹⁵N resonances shift from about 120 ppm in the free ligands to about 160 ppm in the organo-POMs and they do not vary much in the different POMs. Simultaneously, the ¹H signals are also strongly shifted downfield (2 ppm average shift) in the organo-POMs, as mentioned above.

The observation of crosspeaks demonstrates that the target proton remains bound to the amide in the POMs, as does the significant ¹H chemical shift difference between **1a** and **2a,b**. The latter certainly reflects the different magnetic environment of the amide when substituted by a phenyl ring, relative to an electronically different pyridine ring. This difference would likely be less pronounced if the protons were attached to the metal oxide surface, far from the substituents. The strong downfield shift observed in ¹H and ¹⁵N supports our assumption that upon coordination of the amide oxygen to the vanadate atoms the amide assumes a higher imidate character (Figure 1, top right) with a partial positive charge on the nitrogen that is likely responsible for the downfield shifts.

In order to further validate our hypothesis, we performed DFT calculations at the BP86/LANL2DZ level of theory within the Gaussian09 suite of programs^[6] for the protonated and deprotonated hybrid-POM molecules. An implicit solvent correction was added to model the acetonitrile. The example of **1a** is shown in Figure 4. In the protonated form (upper panel, a), the HN-C(Ph)=O bond length was calculated at 1.36 Å, and that of the C=O bond was 1.28 Å. The phenyl group appears slanted and the V-O(=C)-V bridge is distorted, with the V-O bond facing the C-H of the phenyl longer than the V-O bond on the other side (2.26 Å vs. 2.35 Å). The N-C bond connecting the amide group to the diol part is 1.51 Å long. In the deprotonated form (lower panel, b), the N-C(Ph)=O bond length shortens to 1.31 Å, while the C=O bond is lengthened (1.37 Å). The phenyl group is much less slanted, and the V-O(=C)-V bridge is symmetrical (equal V-O bond lengths at 2.13 Å). The N-C bond connecting the amide group to the diol part is unchanged (1.50 Å). This trend is similar for all the systems calculated, including the pyridine derivatives (Table S1 and Figures S1,S2).

We then computed the ¹H NMR chemical shifts of the amide proton of all POMs studied (in their N-protonated forms), using the GIAO protocol, at the PBE1PBE/LANL2DZ//BP86/LANL2DZ level of theory. The calculated values were in very good linear agreement with the observed shifts (Figure S3, R² = 0.952), with a systematic deviation of 0.33 ppm. Finally, we calculated the proton affinities for **1a**. This was carried out to explore the possibility of a protonation on the oxo ligands of the POM structure. The proton affinity

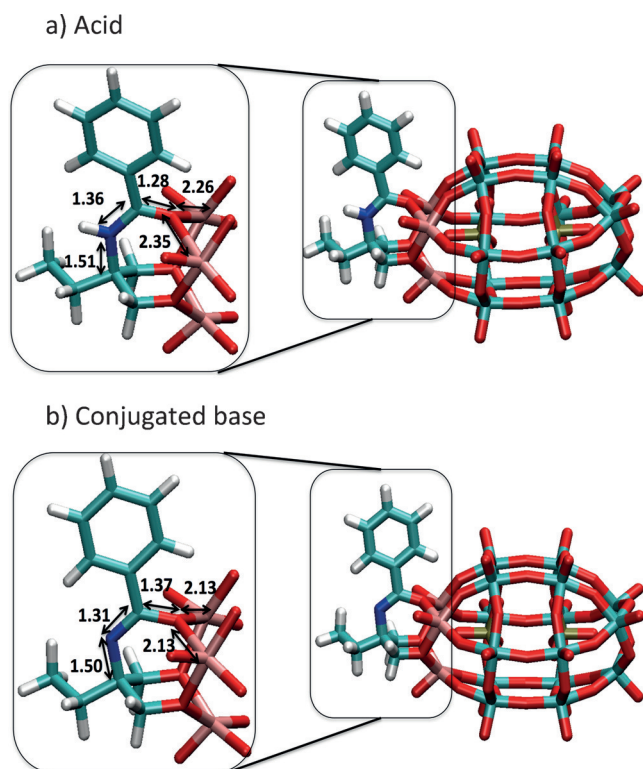


Figure 4. Calculated structure of POM **1a**, fully optimized at the DFT level for the a) *N*-protonated and b) conjugated base forms.

at the nitrogen position is more favorable by at least $25.3 \text{ kcal mol}^{-1}$ compared to a terminal oxygen and by at least $19.5 \text{ kcal mol}^{-1}$ compared to a bridging oxo (Table S2). This means that according to calculations, the POM surface is not basic enough to deprotonate the inserted amide. Similar conclusions can be drawn from all the other systems (see Table S2).

All these models confirm the positioning of the proton on the nitrogen, not on the POM structure. The calculated bond lengths are fully consistent with our hypothesis. In the protonated form, the C–N bond has less double-bond character, and is longer. The C=O bond is also shorter because of the conjugation to the C–N. Steric strain appears between the POM and the phenyl group, which results in a distortion. The organic ligand “pulls” the oxygen to escape this tension, resulting in longer V–O bonds, and a loss of symmetry. Upon deprotonation, the C–N bond is considerably shortened, while the C–O bond is lengthened. This reflects the increase of the imidate form, as expected since more electron density is accommodated on the oxygen, and the POM. The C–O bond lengthening also releases the strain, with a V–O–V crown back to normal.

The electronic nature of the arene substituent influences the NMR chemical shifts. The amide signals in **1b** and **1d** are much further downfield, as one would expect since electron-withdrawing groups are likely to pull electron density from the iminium, thus making the N–H more polarized, while a donating group would do the contrary (as in **1c**). For pyridine-substituted POMs **2a,b**, the signals are even further downfield. This can be a consequence of the presence of the

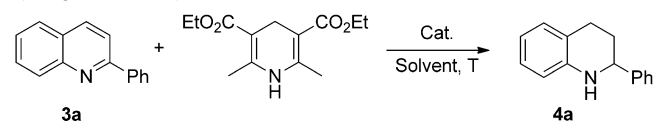
electron-poor heteroaromatic ring, which pull electrons and/or of a difference in anisotropy cones compared to arenes. The natural population analysis conducted on DFT optimized structures indicates no significant variation of the charges redistribution between arenes and pyridines (see Table S3), which tends to support the second argument.

The 1D ^1H spectra of compounds **2a** and **2b** evidenced no extra peak that could indicate the presence of protonated pyridinium ion (i.e. an internal prototropy from the amide to the pyridine ring). No extra peak attributable to protonated pyridinium could be found in the HSQC spectra either, and this was consistent with the chemical shift calculations. However, to exclude the possibility that the pyridinium proton would not be observed because of a rapid exchange with the residual water in the solvent, we acquired 2D ^1H - ^{15}N HMBC spectra (Figure S4). The 2D ^1H - ^{15}N HMBC experiment correlates the nitrogen spin with the non-exchangeable protons attached to the carbon which is bound to nitrogen via the weak long-range ^1H - ^{15}N 2J or 3J -scalar couplings. It is thus possible to determine the ^{15}N chemical shift of the pyridine nitrogen independently of its protonation state and to clearly assess if it is protonated or not. This experiment provides in just a few hours of acquisition an unambiguous confirmation of the pyridine protonation state but also a confirmation of the correct assignment of the amide nitrogen. We observed a correlation among the aromatic proton of the pyridines and the nitrogen resonance at 303.8 ppm for **2a** and 306.6 ppm for **2b**. This chemical shift value is very close to the chemical shift of the free pyridine (302 ppm in CHCl_3) and it is far from the chemical shift observed for the protonated pyridinium ions (204 ppm in CHCl_3 for the pyridinium chlorohydrate).^[7] This unambiguously shows that the pyridine is not protonated in organo-POMs **2a** and **2b**.

The absence of prototropy in **2a,b** suggests that the protons of the inserted amide are only weakly acidic. To evaluate the potential of the organohybrids as Brønsted organocatalysts we thus targeted a reaction where the key event does not involve protonation of the weakly basic carbonyl group. The organo-catalyzed reduction of quinolines appeared as a perfect benchmark.^[8] The mechanism of that reaction involves the formation of an ion pair between the deprotonated form and the protonated quinoline substrate. The latter is then hydrogenated by the Hantzsch ester. We felt that the highly negative charge of the POM would ensure the formation of a tight ion pair, potentially giving it a stronger influence over the course of the reaction.

In a first experiment, we heated a suspension of POM **1a** (1 mol %), 2-phenyl quinoline **3a**, Hantzsch ester (2.5 equiv) in toluene for 13 h (Table 1, entry 1). Gratifyingly, 62 % of the expected **4a** were isolated. No reaction took place in THF (entry 2), but the reaction was quantitative in acetonitrile (entry 3). We selected this solvent for the rest of the study. At room temperature the reaction was slower, taking 3 days to yield 68 % of **4a** (entry 4). With 0.5 mol % of catalyst, the yield was 94 % (entry 5). With 0.1 mol % of catalyst, the conversion suffered and only 30 % of **4a** was isolated (entry 6).

We next carried out control experiments. No reaction took place in the absence of POM (entry 7), or in the presence of

Table 1: Optimization of the conditions for the organo-POM-catalyzed hydrogenation of quinolines.


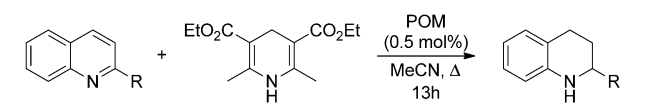
Entry ^[a]	Cat. (mol %)	Solvent	T	Yield [%]
1	1a (1)	toluene	Δ	62
2	1a (1)	THF	Δ	— ^[b]
3	1a (1)	MeCN	Δ	99
4	1a (1)	MeCN	RT	68 ^[c]
5	1a (0.5)	MeCN	Δ	94
6	1a (0.1)	MeCN	Δ	30
7	—	MeCN	Δ	— ^[b]
8	TBABr	MeCN	Δ	— ^[b]
9	diolamide (R = Ph, 0.5)	MeCN	Δ	— ^[b]
10	TBA ₅ H ₄ [P ₂ W ₁₅ V ₃ O ₆₂] (0.5)	MeCN	Δ	62
11	TBA _{6.5} H _{2.5} [P ₂ W ₁₅ V ₃ O ₆₂] (0.5)	MeCN	Δ	34
12	TBA ₅ H ₄ [P ₂ W ₁₅ V ₃ O ₆₂] (0.5) + diolamide (R = Ph, 0.5)	MeCN	Δ	59

[a] Unless otherwise noted: 2-phenylquinoline (1 equiv), Hantzsch ester (2.5 equiv), reaction left for 13 h. [b] No reaction. [c] Reaction was left for 3 days.

tetrabutylammonium bromide (entry 8). The “free” diolamide alone did not catalyze the reaction either (entry 9). On the other hand, the purely inorganic [P₂W₁₅V₃O₆₂]^{9−} surrounded by five TBA⁺ cations and four protons delivered 62 % of **4a** (entry 10). After cation exchange on a TBA-loaded resin to strip it from some of its surrounding protons, the activity of the same POM (with 6.5/2.5 TBA⁺/H⁺ counterions) dropped significantly (34 % completion after 13 h, entry 11). Finally, the physical mixture of TBA₅H₄[P₂W₁₅V₃O₆₂] and the diolamide (thus with no covalent attachment) returned a yield comparable to that of TBA₅H₄[P₂W₁₅V₃O₆₂] alone (59 %, entry 12).

The controls show that the POM is necessary for the reaction to proceed. As one would expect from the literature, the diolamide in itself is not capable of acting as a protic catalyst, nor is the POM counterion. The experiments of entries 10–11 show that the purely inorganic structure is a possible catalyst because of its surrounding protons. However, with four protons it is already less active than **1a**, and its activity drops further with the proton concentration. As the full deprotonation of **1a** would provide a species with only one proton, we can surmise that the latter would be even less active. Finally, there is no cooperativity of the inorganic and organic partners if they are not grafted (entry 12). As the NMR shows that the proton of the amide is on the nitrogen, and not on the POM surface we deduce that the activity stems from the activation of the amide in the grafted species. The inorganic structure does not act as a support for a proton, like the usual heteropolyacids, but it exalts the acidity of the organic part.

We next shortly examined the influence of changes in the POM structure and in the substrate. Given the molecular weight of the POM, we selected the conditions of entry 5 for a short scope study (Table 2). Compared to the previously

Table 2: Scope of the hydrogenation.


Entry	Substrate	POM	Product, yield [%]
1	3a	1a	4a , 94
2	3a	1b	4a , 91
3	3a	1d	4a , 96
4	3a	1c	4a , 81
5	3b	1a	4b , 95
6	3c	1a	4c , 100
7	3d	1a	4d , 100

optimized reaction (Table 2, entry 1), both POMs with electron-withdrawing substituents **1b** and **1d** led to similarly high yields of **4a** (entries 2,3). Hybrid **1c** which has a donating *para*-methoxy substituent was slightly less efficient (81 % vs. 94 with **1a**, entry 4). On the substrate side, all substrates considered led to an efficient reaction (entries 5–7). This rapid scope study shows that the POM-based catalyst tolerates changes in the periphery of the inserted amide, providing an opportunity for tuning.

To summarize, we have introduced a new family of acidic POMs, in which the acidity of an amide proton is exalted upon grafting to the vanadium-oxide crown of a Dawson vanadotungstate. Cooperative interactions between the inorganic and organic parts of the organo-POM lead to the first covalent hybrid heteropoly acids.^[5b–c,9] Beyond POM chemistry, this is a new way of generating acidic organocatalysts, a subclass of catalysts with a rather narrow functional diversity. The organic end could be further decorated to enhance the activity or build a chiral pocket around the proton.

Acknowledgements

This work was supported by CNRS, the Région Rhône-Alpes (doctoral stipend to D.V.), CPE Lyon, Université Claude Bernard Lyon 1, ENS Lyon and TGIR RMN-THC FR 3050 (CRMN-Lyon). We thank the Pôle Scientifique de Modélisation Numérique at ENS-Lyon for modeling time.

Keywords: acid derivatives · hydrogen transfer · organic-inorganic hybrid composites · organocatalysis · polyoxometalates

How to cite: *Angew. Chem. Int. Ed.* **2016**, *55*, 5961–5965
Angew. Chem. **2016**, *128*, 6065–6069

- [1] a) S.-S. Wang, G.-Y. Yang, *Chem. Rev.* **2015**, *115*, 4893; b) V. F. Odyakov, E. G. Zhizhina, Y. A. Rodikova, L. L. Gogin, *Eur. J. Inorg. Chem.* **2015**, 3618; c) I. Kozhevnikov in *Handbook of*

- Green Chemistry*, Vol. 2 (Eds.: P. T. Anastas, R. H. Crabtree), Wiley-VCH, Weinheim, **2009**, pp. 153–174.
- [2] a) D. Hueber, M. Hoffmann, B. Louis, P. Pale, A. Blanc, *Chem. Eur. J.* **2014**, *20*, 3903; b) D. Hueber, M. Hoffmann, P. de Fremont, P. Pale, A. Blanc, *Organometallics* **2015**, *34*, 5065; c) N. Dupré, P. Remy, K. Micoine, C. Boglio, S. Thorimbert, E. Lacôte, B. Hasenknopf, M. Malacria, *Chem. Eur. J.* **2010**, *16*, 7256; d) Q. Han, C. He, M. Zhao, B. Qi, J. Niu, C. Duan, *J. Am. Chem. Soc.* **2013**, *135*, 10186; e) Y. Kikukawa, K. Suzuki, M. Sugawa, T. Hirano, K. Kamata, K. Yamaguchi, N. Mizuno, *Angew. Chem. Int. Ed.* **2012**, *51*, 3686; *Angew. Chem.* **2012**, *124*, 3746; f) K. J. Stowers, K. C. Fortner, M. S. Sanford, *J. Am. Chem. Soc.* **2011**, *133*, 6541.
- [3] a) M.-P. Santoni, G. S. Hanan, B. Hasenknopf, *Coord. Chem. Rev.* **2014**, *281*, 64; b) H. Li, L. Wu, *Soft Matter* **2014**, *10*, 9038; c) A. Dolbecq, E. Dumas, C. R. Mayer, P. Mialane, *Chem. Rev.* **2010**, *110*, 6009; d) P. Yin, D. Li, T. Liu, *Chem. Soc. Rev.* **2012**, *41*, 7368; e) A. Proust, R. Thouvenot, P. Gouzerh, *Chem. Commun.* **2008**, 1837; f) D.-L. Long, R. Tsunashima, L. Cronin, *Angew. Chem. Int. Ed.* **2010**, *49*, 1736; *Angew. Chem.* **2010**, *122*, 1780.
- [4] a) S. Luo, J. Li, H. Xu, L. Zhang, J.-P. Cheng, *Org. Lett.* **2007**, *9*, 3675; b) J. Li, X. Li, P. Zhou, L. Zhang, S. Luo, J.-P. Cheng, *Eur. J. Org. Chem.* **2009**, 4486.
- [5] a) J. Li, I. Huth, L.-M. Chamoreau, B. Hasenknopf, E. Lacôte, S. Thorimbert, M. Malacria, *Angew. Chem. Int. Ed.* **2009**, *48*, 2035; *Angew. Chem.* **2009**, *121*, 2069; b) B. Riflade, A. Noël, M. Malacria, S. Thorimbert, B. Hasenknopf, E. Lacôte, *Org. Lett.* **2011**, *13*, 5990; c) B. Riflade, D. Lachkar, J. Obie, J. Li, S. Thorimbert, B. Hasenknopf, E. Lacôte, *Org. Lett.* **2014**, *16*, 3860; d) I. Azcarate, I. Ahmed, R. Fara, M. Goldmann, X. Wang, H. Xu, B. Hasenknopf, E. Lacôte, L. Ruhlmann, *Dalton Trans.* **2013**, *42*, 12688; e) I. Azcarate, Z. Huo, R. Farha, M. Goldmann, H. Xu, B. Hasenknopf, E. Lacôte, L. Ruhlmann, *Chem. Eur. J.* **2015**, *21*, 8271. The polyoxoanion can also be converted into its triester derivative. See: f) Y. Hou, C. L. Hill, *J. Am. Chem. Soc.* **1993**, *115*, 11823; g) C. P. Pradeep, D.-L. Long, G. N. Newton, Y. F. Song, L. Cronin, *Angew. Chem. Int. Ed.* **2008**, *47*, 4388; *Angew. Chem.* **2008**, *120*, 4460; h) Y. Han, Y. Xiao, Z. Zhang, B. Liu, P. Zheng, S. He, W. Wang, *Macromolecules* **2009**, *42*, 6543.
- [6] Gaussian09, Revision D.01, M. J. Frisch, et al., Gaussian, Inc., Wallingford CT, **2009**.
- [7] R. O. Duthaler, J. D. Roberts, *J. Am. Chem. Soc.* **1978**, *100*, 4969.
- [8] a) M. Rueping, A. P. Antonchick, T. Theissmann, *Angew. Chem. Int. Ed.* **2006**, *45*, 3683; *Angew. Chem.* **2006**, *118*, 3765; b) J. W. Yang, M. T. Hechavarria Fonseca, B. List, *Angew. Chem. Int. Ed.* **2004**, *43*, 6660; *Angew. Chem.* **2004**, *116*, 6829; c) C. Zhu, T. Akiyama, *Org. Lett.* **2009**, *11*, 4180.
- [9] For other examples of organo-POM catalysts, see: a) C. Brazel, N. Dupré, M. Malacria, B. Hasenknopf, E. Lacôte, S. Thorimbert, *Chem. Eur. J.* **2014**, *20*, 16074; b) G. Modugno, A. Monney, M. Bonchio, M. Albrecht, M. Carraro, *Eur. J. Inorg. Chem.* **2014**, 2356; c) W.-K. Miao, Y.-K. Yan, X.-L. Wang, Y. Xiao, L.-J. Ren, P. Zheng, C.-H. Wang, L.-X. Ren, W. Wang, *ACS Macro Lett.* **2014**, *3*, 211; d) M. Carraro, G. Fiorani, L. Mognon, F. Caneva, M. Gardan, C. Maccato, M. Bonchio, *Chem. Eur. J.* **2012**, *18*, 13195; e) N. Dupré, C. Brazel, L. Fensterbank, M. Malacria, S. Thorimbert, B. Hasenknopf, E. Lacôte, *Chem. Eur. J.* **2012**, *18*, 12962; f) S. Berardi, M. Carraro, M. Iglesias, A. Sartorel, G. Scorrano, M. Albrecht, M. Bonchio, *Chem. Eur. J.* **2010**, *16*, 10662; g) I. Barnahum, R. Neumann, *Chem. Commun.* **2003**, 2690; h) H. Zeng, G. R. Newkome, C. L. Hill, *Angew. Chem. Int. Ed.* **2000**, *39*, 1771; *Angew. Chem.* **2000**, *112*, 1841.

Received: November 25, 2015

Revised: February 26, 2016

Published online: April 8, 2016